

Non-linear static analysis (Push-over) and inelastic analysis of 3-story, 6-story, 9-story and 17-story RC buildings of ductile frames designed in Mexico City for different permissible lateral deformation levels



J. A. Avila, J. C. Manzano & L. A. Villegas

Institute of Engineering, National University of Mexico (UNAM), Mexico

SUMMARY:

With 3, 6, 9 and 17-story RC buildings of ductile frames, previously designed, non-linear static analysis with increased monotonically lateral loads (Push-over) are made in order to determine its collapse and their responses against the inelastic dynamic seismic analysis results with the SCT-EW-85 record are compared. It is designed with the Appendix A condition of the Seismic Technical Norms of the Mexico City Code (RDF-04), satisfying the maximum story distortion limits of the service and collapse conditions; the buildings (offices) are in the III_b compressible seismic zone. The non-linear responses were determined with nominal resistance and over-resistance effects. For the non-linear static analysis was important to select the type of lateral forces distribution. The comparison were made with curves of base shear force–roof lateral displacement, global distribution of plastic hinges, failure mechanics tendency, lateral displacements and story drifts, local and global ductility demands, etc.

Keywords: Non-linear static analysis; inelastic dynamic seismic analysis

1. INTRODUCTION

In this work, it is determined and compared the non-linear seismic (Push-Over) and the dynamic inelastic step by step behavior in 3, 6, 9 and 17-story buildings with reinforced concrete (RC) frames located in the compressible zone of México City. The design is made with the Mexico City Code (RDF-04, 2004), according to the service and failure limit states established in its corresponding Complementary Techniques Norms (CTN-Seismic and CTN-Concrete). The structures were designed as follows: A) with the design spectrum of the Main Body (MB) of the CTN-Seismic (seismic zone III_b); B) with the design spectrum according to the soil dominant period, defined in the Appendix A of the CTN-Seismic ($T_s = 2$ seconds). The inelastic seismic responses in time history were analyzed with the records representative of maximum compressible soil damage in Mexico City during the earthquake of September 1985. For the Push-Over analyses, the responses under different lateral load distributions were calculated and the collapse mechanisms, curves base shear force–roof lateral displacement and the maximum demands of local and global ductility were determined. It is included the influence of the possible over-resistance sources. With the results of this work it is to show that there are no important variations between Main Body and Appendix A cases. The Appendix A criterion allows to determinate displacement of the conditions of service and collapse to the structure may be subject.

2. ELASTIC RESPONSE CALCULATION

2.1. Structures description and design procedure

They are office buildings of 3, 6, 9 and 17-story of reinforced concrete, symmetric and regular in plan and elevation. They have a foundation rigid box. The 9-story building has friction piles and the 17-

story building has point piles; for the first one the base flexibility effects are considered. The concrete is class 1 with $f'_c = 250 \text{ kg/cm}^2$ and elastic modulus $E_c = 14,000$ times square root of f'_c , and the longitudinal and transverse steel with $f_y = 4,200 \text{ kg/cm}^2$. The structural system is formed with reinforced concrete frames by girders and columns rigidly connected by a solid slab of 10 cm thick. Fig. 2.1. shows the principal details in plan and elevation of the buildings under study. The column and girder resistances were designed for the last mechanic elements of the spectral modal dynamic analysis, considering the three-dimensional structural performance more the vertical load effects (dead loads and live loads) and second order effects, and for the ductile frame special requirements established by Concrete Norms, due to the use of seismic performance factors $Q = 4$ for 3 and 6-story buildings, and $Q = 3$ for 9 and 17-story buildings.

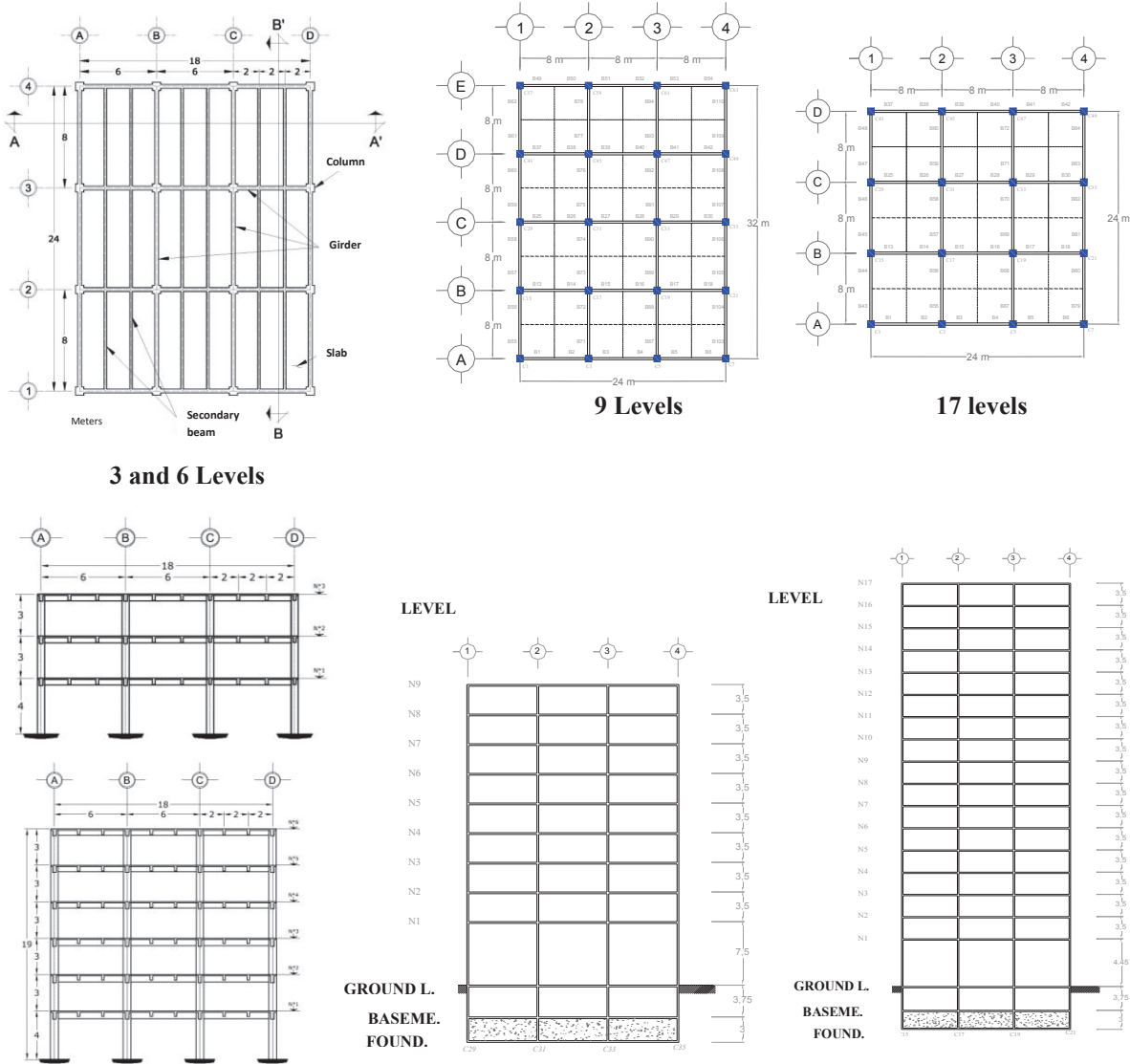


Figure 2.1. Structural plant-type (dimensions in meters) and transversal cuts of 3, 6, 9 and 17-story buildings

2.2. Vibrations periods

Table 2.1. compares the three periods of vibration modes (directions X, Y and θ) of the 3, 6, 9 and 17-story buildings, respectively. There are no differences between Main Body and Appendix A cases, as expected. For 17-story building, due to the symmetry of the structure, periods in the direction X and Y are the same. Figs. 2.2. and 2.3. show the design spectra of the RDF-04 of the Main Body (seismic zone III_b) and the Appendix A ($T_s = 2$ seconds), the elastic and inelastic response spectra of record

SCT-EW-85 (critical viscous damping of 5%) as well as the location of the fundamental periods of vibration of the 3 ($T_{1x} = 0.663$ seconds), 6 ($T_{1x} = 0.832$ seconds), 9 ($T_{1x} = 1.502$ seconds) and 17-story buildings ($T_{1x} = 1.752$ seconds) in the direction X.

Table 2.1. Vibration periods of 3, 6, 9 and 17-story buildings

Vibration periods, T_i (seconds)												
Direction	3-story			6-story			9-story			17-story		
	T_1	T_2	T_3	T_1	T_2	T_3	T_1	T_2	T_3	T_1	T_2	T_3
X	0.663	0.180	0.081	0.832	0.279	0.138	1.502	0.563	0.335	1.752	0.643	0.374
Y	0.674	0.182	0.081	0.837	0.278	0.138	1.460	0.551	0.332	1.752	0.643	0.374
θ (torsion)	0.536	0.147	0.066	0.676	0.228	0.114	1.132	0.420	0.254	1.346	0.518	0.306

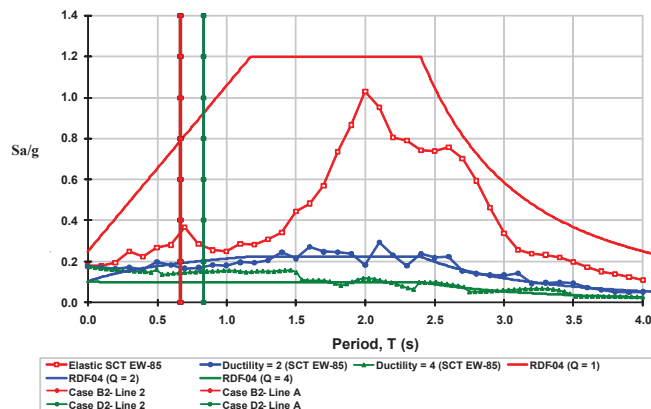


Figure 2.2. Location of fundamental periods of vibration of the 3 and 6-story structures, regarding the design spectra ($Q=1$ y 4) of Appendix A (cases B2 and D2) and the response spectra ($\mu=1$ y 4) of SCT-EW-85 record

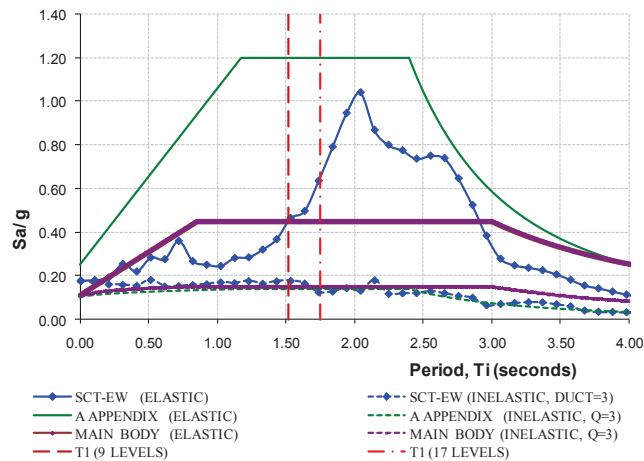


Figure 2.3. Location of fundamental periods of vibration of the 9 and 17-story structures, regarding the design spectra ($Q=1$ y 3) and the response spectra ($\mu=1$ y 3) of SCT-EW-85 record

2.3. Maximum story drifts

The 3-story building under earthquake in both directions, accomplishes with the permissible limit of 0.006 specified in the Main Body, and with the permissible limit of 0.002 for Appendix A; the collapse limit of 0.03 was not a condition to govern the performance of the design. The 6-story

building accomplishes with both permissible limits (service condition); the story drifts in this structure are closer to the collapse limit than the 3-story model. The 9-story building accomplishes with the permissible limit of 0.012 specified in the Main Body, and it is lightly above the limit of 0.004 of Appendix A; the collapse limit of 0.03 was not a condition to govern the behavior of the design of the building. The 17-story building accomplishes with both permissible limits, be a little above the condition of service of Appendix A (see Fig. 2.4).

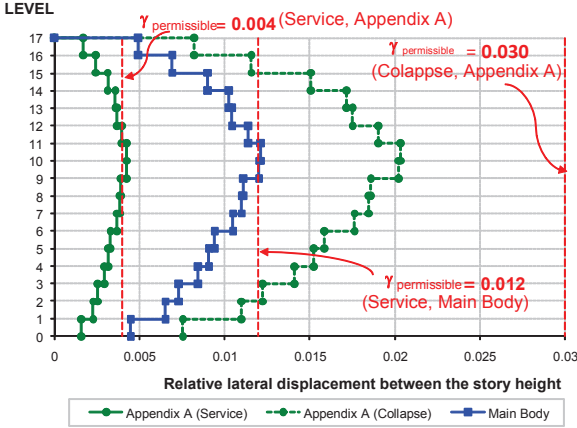


Figure 2.4. Maximum story drifts under X and Y directions earthquake, spectral modal dynamic seismic analysis, 17-story building

3. CALCULATION OF THE INELASTIC DYNAMIC RESPONSE

Inelastic dynamic responses step-by-step are determined by using the SCT accelerogram, E-W component, registered on September 19th 1985. The responses were calculated for the lines 2 (direction X) and A (direction Y) of the 3-story and 6-story buildings, lines C and B for the 9 and 17-story buildings, respectively; such frames were “calibrated” to ensure static and dynamic behavior similar to the three-dimensional model.

3.1. Global ductility maximum demands, μ_G

All cases of 3, 6, 9 and 17-story buildings, with nominal resistances, experiment inelastic performance; generally the models with over-resistance effects have lower global ductility demands. In no case μ_G was over 4 or 3, equal to the value of the seismic performance factor (Q) with which the elastic design spectra were reduced (see table 3.1.).

Table 3.1. Calculated global ductility maximum demands of 3, 6, 9 and 17-story buildings under inelastic step-by-step seismic analysis with nominal and over-resistances

Nominal resistance				Over-resistance		
Levels	Δ_Y (cm)	$\Delta_{max\ inelastic}$ (cm)	μ_G	Δ_Y (cm)	$\Delta_{max\ inelastic}$ (cm)	μ_G
3 (Q= 4)	1.86	4.12	2.22	3.33	4.02	1.21
6 (Q= 4)	5.23	18.44	3.53	5.16	5.91	1.15
9 (Q= 3)	14.34	37.57	2.62	20.52	33.23	1.62
17 (Q= 3)	19.24	42.85	2.23	29.01	47.01	1.62

$\mu_G = \Delta_{max\ inelastic} / \Delta_Y$; Δ_Y = roof lateral displacement for the first yield; $\Delta_{max\ inelastic}$ = roof maximum lateral displacement for the inelastic performance.

3.2. Curves of base shear force–roof lateral displacement

When an inelastic behavior is present, it is observed that, as the structure dissipates more amount of seismic energy, the responses have more hysteretic area, and there are further reductions in the base shear force and the roof horizontal displacement. Figs. 3.1. to 3.4. compare the base shear force–roof lateral displacement relationship of the 3, 6, 9 and 17-story buildings under elastic and inelastic step-by-step seismic analysis with nominal and over-resistances. The hysteretic curves of the 9-story model present light wider, which means light larger raid in the nonlinear range and higher energy dissipation; the over-resistance cases tend to behave elastically. The 17-story models tend to have a larger hysteretic area, and over-resistance cases show a light inelastic behavior, although on a less important way that the condition of nominal resistance.

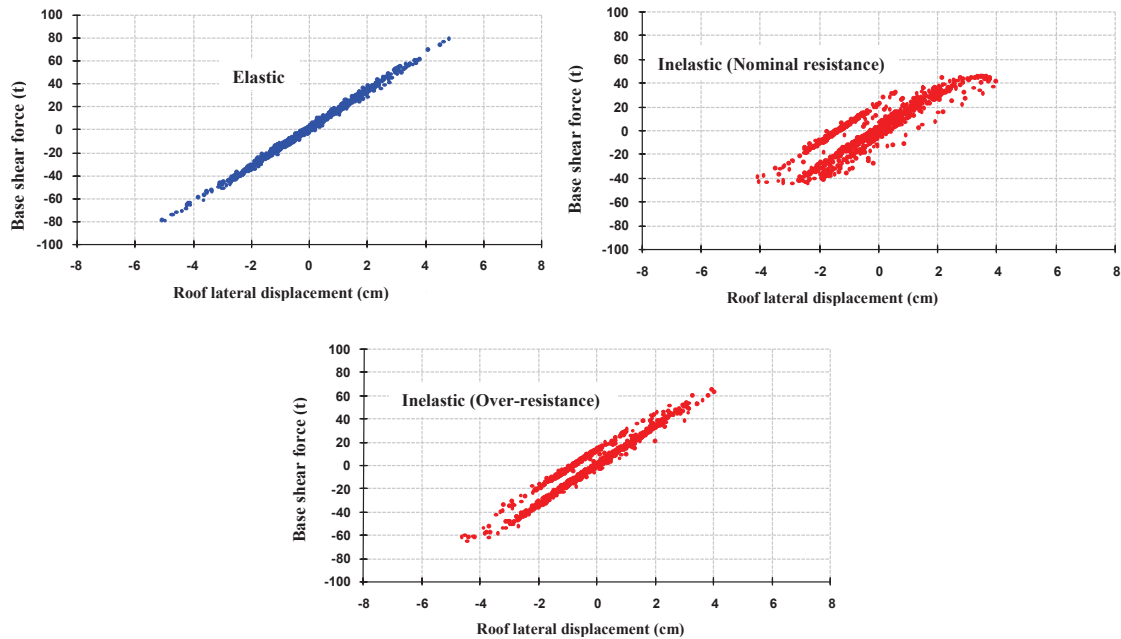


Figure 3.1. Curves of base shear force–roof lateral displacement, elastic and inelastic step-by-step seismic analysis (nominal and over-resistances), 3-story structure

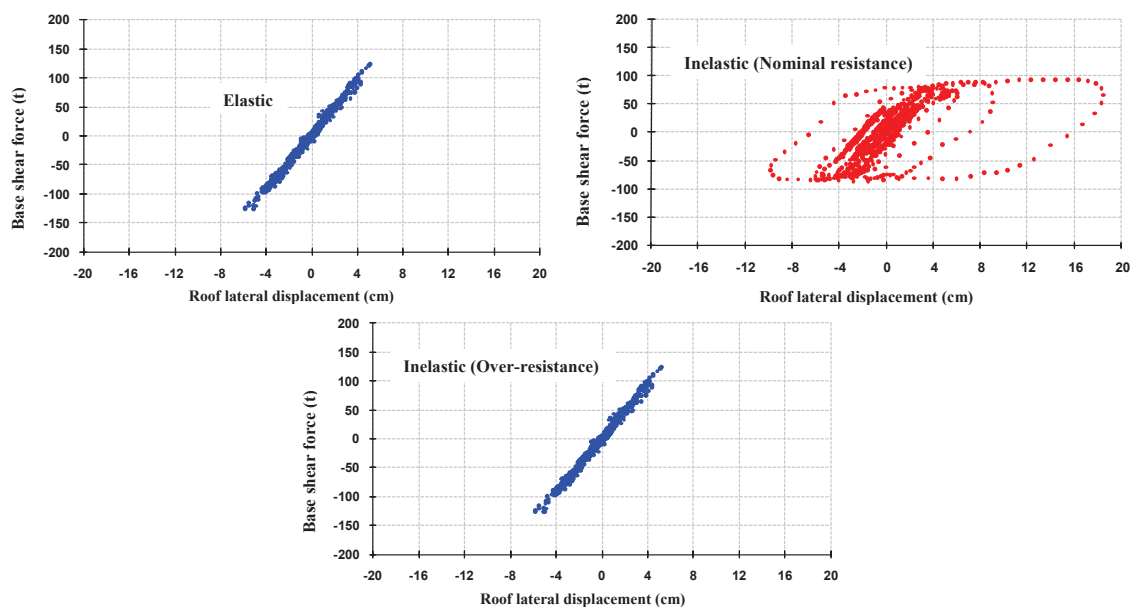


Figure 3.2. Curves of base shear force–roof lateral displacement, elastic and inelastic step-by-step seismic analysis (nominal and over-resistances), 6-story structure

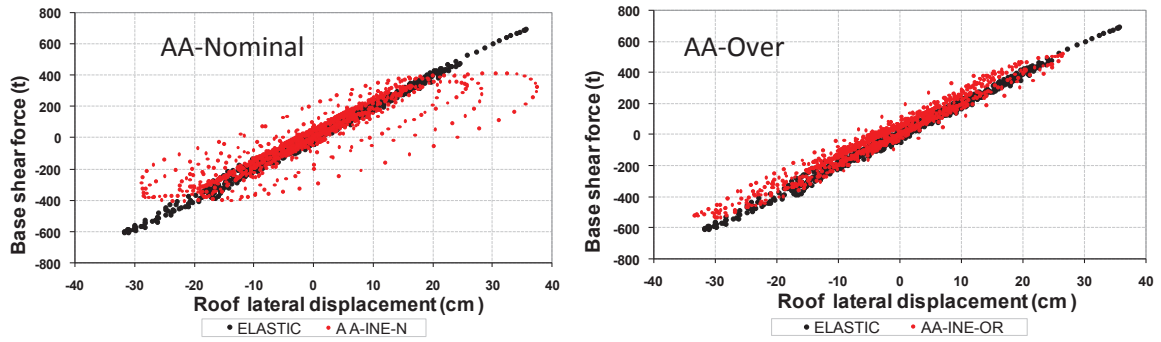


Figure 3.3. Curves of base shear force–roof lateral displacement, elastic and inelastic step-by-step seismic analysis (nominal and over-resistances), 9-story structure

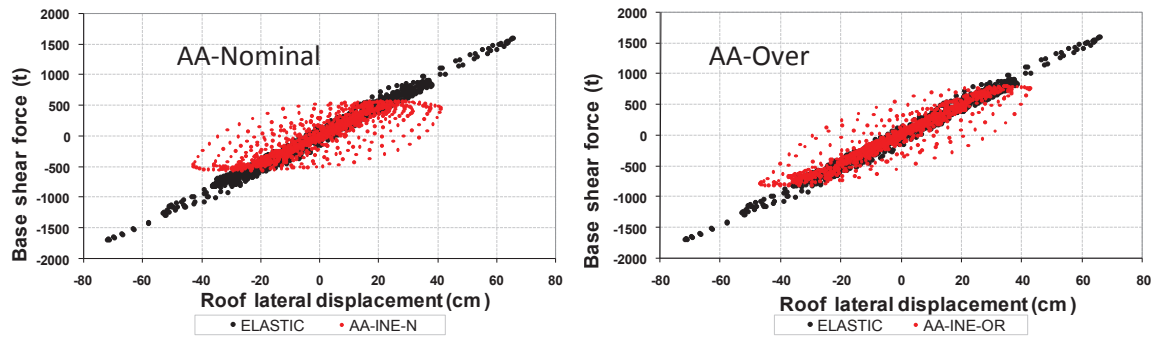


Figure 3.4. Curves of base shear force–roof lateral displacement, elastic and inelastic step-by-step seismic analysis (nominal and over-resistances), 17-story structure

3.3. Global distribution of plastic hinge and demands of local ductility

In all buildings, the overall distribution of plastic hinges had a general tendency to the failure mechanism known as a "beam" type; this is, the plastic hinges are present in most of the beams and columns only in some, which is consistent with the design philosophy of "strong column-weak beam" of the RDF-04 code. Fig. 3.5. has global distributions of plastic hinges on the 9-story building without and with over-resistances. Colors described different times in which each plastic hinge was introduced from blue color in the beginning until the end of the most intensive phase of the record SCT-EW-85, using in these cases the step-by-step analyses. Fig. 3.6. shows the maximum local ductility demands developed in beams, for Main Body and Appendix A conditions of the 9 and 17-story buildings in study; columns behave almost in the elastic range, with maximum demands less than 1.5. The maximum demands for the nominal cases are values between 4 and 6 in beams, whereas in columns, the values are less than 2; with the over-resistance effects, such that the maximum demands in beams are from 2 to 3 and columns behave elastically, for practical purposes. The maximum value in beams in the 17-story building varies between 3 and 7 with nominal resistance and between 1.5 and 3 when over-resistance effects are considered.

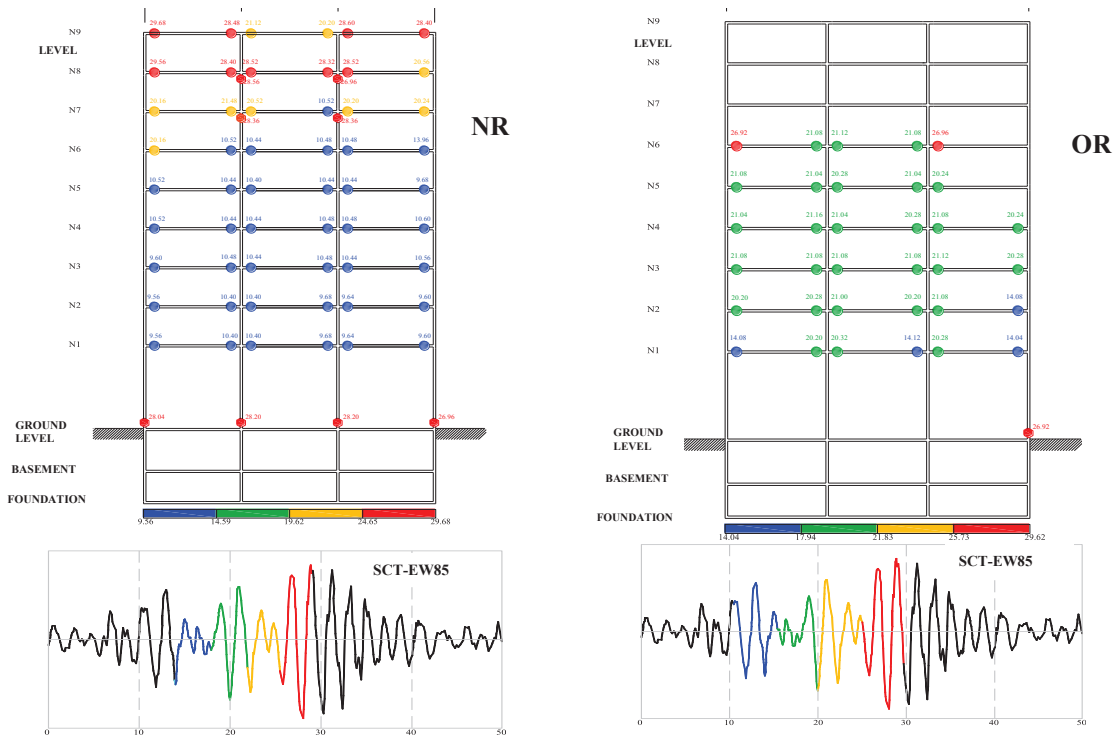


Figure 3.5. Appartition sequence and global distribution of plastic hinges, 9-story structure, with nominal resistances (NR) and over-resistances (OR) effects

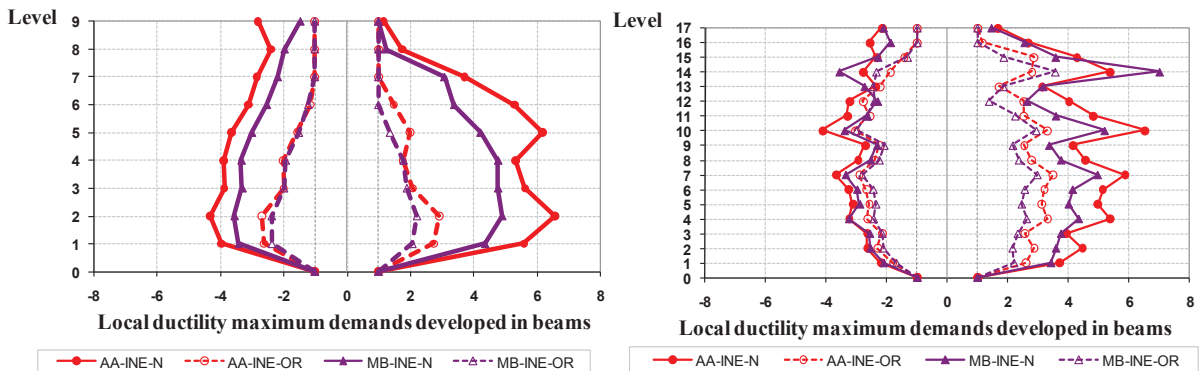


Figure 3.6. Local ductility maximum demands developed in beams, inelastic step by step analysis with nominal resistances (N) and over-resistances (OR), 9 and 17-story buildings, Main Body and Appendix A designs

4. NON-LINEAR STATIC ANALYSIS (PUSH-OVER)

The non-linear static analysis with four different distributions of lateral load, were made without and with the over-resistance effects, to know: 1) SMD distribution with forces at the floor level (F_i), determined from the story shear forces (V_i) from spectral modal dynamic analysis, involving all modes of lateral vibration; 2) Elastic step-by-step distribution with forces at floor level (F_i), calculated with the story shear forces (V_i) for a “ t_i ” time from an step-by-step analysis, when the structure is working in the elastic range; 3) Inelastic step-by-step distribution with forces at floor level (F_i), defined with the story shear forces (V_i) for a “ t_i ” time from an step-by-step analysis when the structure the maximum inelastic roof displacement is shown; 4) Linear triangular distribution from F_i forces as a result of the hypothesis of static seismic analysis (linear). Fig. 4.1. shows the laterals loads distributions for the non-linear static analysis (Push-over) of the 17-story building. The results shown are only for the case in which the distributions are obtained from a spectral modal dynamic

analysis (SMD), with the participation of all modes of lateral vibration. The Push-over analyses were made to the following conditions: a) maximum demands of the local ductility in beams are equal to 35, b) maximum demands of the local ductility in columns are equal to 20, c) maximum story drift of the collapse condition is 0.03, according to Appendix A of the CTN-Seismic of RDF-04 Code for structures for ductile concrete frames with $Q=3$ or 4, d) the mechanism of collapse of the structure is reached.

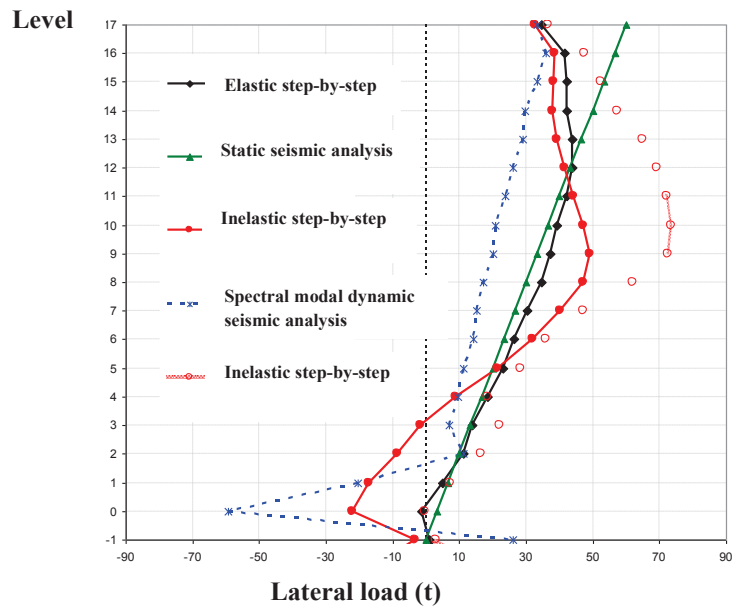


Figure 4.1. Lateral loads distributions for the non-linear static analysis (Push-over), 17-story building

4.1. Curves of base shear force–roof lateral displacement

Figs. 4.2. to 4.5. compare the results of the base shear force–roof lateral displacement relationships of the Push-over analyses against relationship of the corresponding inelastic step-by-step analyses without and with over-resistance effects, of the 3, 6, 9 and 17-story models, designed with Appendix A. In the 3-story building, maximum displacement did not exceed 30 cm, due to the regulation of the limit condition previously established of maximum demands of ductility in columns of 20. For 6-story models, the resulting performance from Push-over analysis was governed generally by the condition of permissible drift of collapse of 0.03. In the 9-story models with nominal resistances, maximum displacement did not exceed 60 cm, due to the regulation of the limit condition previously established of maximum demands of ductility in columns of 20. For 17-story models, the resulting behavior from Push-over analysis was governed generally by the condition of permissible drift of collapse of 0.03. The influence of over-resistance effects is very important. With the results of both types of analysis, confirms what the lateral stiffness and lateral resistance of each structure as well as their capacity of energy dissipation facing the typical seismic effects of Mexico City.

5. CONCLUSIONS

Buildings designed with the Seismic Technical Norms of the Mexico City Code (RDF-04) show satisfactory performance, with enough reserve of resistance, to avoid brittle failure. Significant variations between the designs of the Main Body and Appendix A conditions are not presented. With the help of the over-resistance effects, the maximum responses tended to be lower. The tendency of plastic hinges from step-by-step and non-linear static (Push-over) analyses show, in general, a strong column-weak girder performance according to the current design philosophy, which ensures a ductile

behavior. The Push-over analysis results show consistency regarding to responses of dynamic analysis in time history.

REFERENCES

Gaceta Oficial del Gobierno del Distrito Federal (2004), “Reglamento de Construcciones de la ciudad de México y Normas Técnicas Complementarias para Diseño por Sismo, y para Diseño y Construcción de Estructuras de Concreto”.

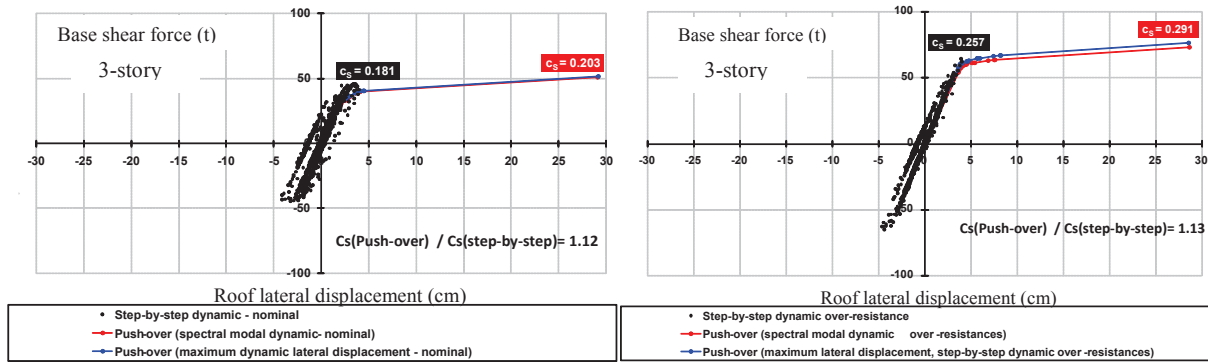


Figure 4.2. Curves of base shear force–roof lateral displacement comparison, non-linear static analysis (Push-over) and inelastic step-by-step dynamic analysis with nominal resistance and over-resistances effects, 3-story structures

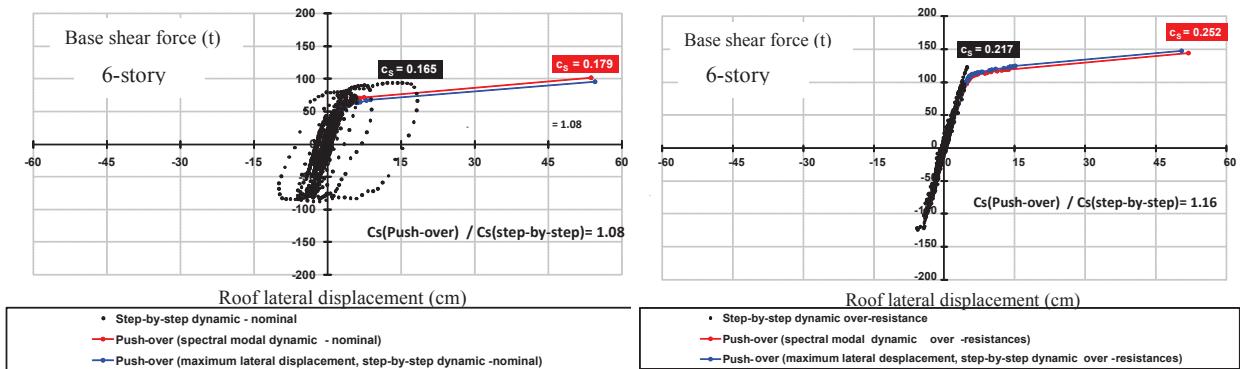


Figure 4.3. Curves of base shear force–roof lateral displacement comparison, non-linear static analysis (Push-over) and inelastic step-by-step dynamic analysis with nominal resistance and over-resistances effects, 6-story structures

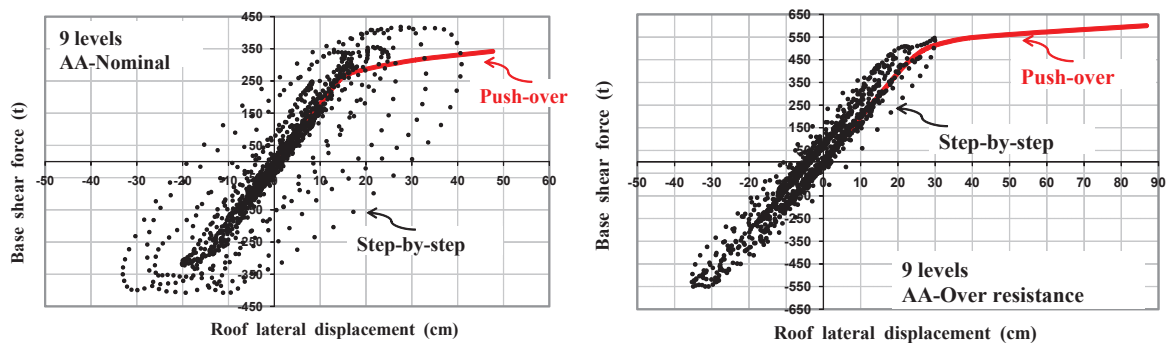


Figure 4.4. Curves of shear force–roof lateral displacement relationships comparison, non-linear static analysis (Push-over) and inelastic step-by-step dynamic analysis with nominal resistance and over-resistances, 9-story structures

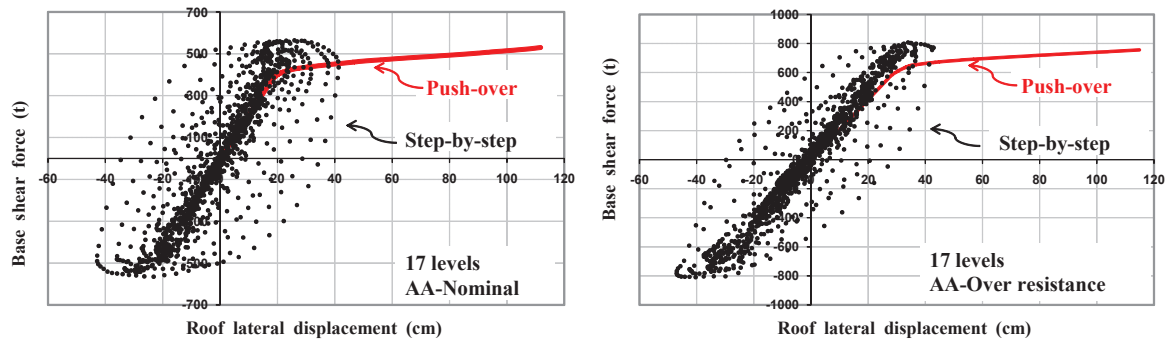


Figure 4.5. Curves of shear force–roof lateral displacement relationships comparison, non-linear static analysis (Push-over) and inelastic step-by-step dynamic analysis with nominal resistance and over-resistances, 17-story structures